Journal of Petroleum Research and Studies

journal homepage: https://jprs.gov.iq/index.php/jprs/

Print ISSN 2220-5381, Online ISSN 2710-1096

Study the Effect of Active Metal Loading within a γ-Alumina Support on Product Distribution in n-heptane Hydroisomerization Reactions

Mohammed Khalil[1*], Zaidoon M. Shakor[1], Bashir Y. Al-Zaidi[1], Sattar J. Hussein[2]

[1]Department of Chemical Engineering, University of Technology, Baghdad, Iraq.
[2]Petroleum Research and Development Center, Ministry of Oil, Baghdad, Iraq.
[*]Corresponding Author E-mail: che.20.08@grad.uotechnology.edu.iq

Article Info

Received 17/12/2023
Revised 08/10/2025
Accepted 23/10/2025
Published 21/12/2025

DOI:
http://doi.org/10.52716/jprs.v15i4.839

Abstract

In this paper, the monofunctional acidic γ-Al_2O_3 catalyst was treated with Pt metals with a percentage ranging from 0.5 to 1 wt% to obtain a bifunctional nanocatalyst represented by Pt/Al_2O_3, for the purpose of increasing the active metal sites on its surface, and thus enhancing the extremely important hydrogenation/dehydrogenation reactions in catalyzing hydroisomerization reactions of *n*-heptane with an octane number of zero. Experiments were conducted in a pilot unit at a temperature of 230°C and under a pressure of 5 bar in the presence of H_2-gas for the purpose of producing desirable fuel hydrocarbons with a high octane number. A number of characterization techniques, including XRD, SEM, EDX, BET and FTIR, have been used to evaluate the physical properties of the catalysts. The catalytic behavior of the prepared catalysts was compared by calculating the conversion of the hydrocarbons formed and the selectivity towards the generation of isomers in the reaction products. The comparison results indicated that the conversion, selectivity and yield track the following order according to the catalytic efficiency of the catalysts: 0.5wt% Pt/Al_2O_3 > 1wt% Pt/Al_2O_3 > γ-Al_2O_3. The highest conversion, selectivity, and yield were found on the surface of the 0.5wt% Pt/Al_2O_3 catalyst, which are 62.50, 80.96, and 50.60 wt%, respectively, while the lowest weight percentages of products were found on the surface of the unloaded-parent γ-Al_2O_3 catalyst, which are 52.8, 67.7, and 35.75 for conversion, selectivity, and yield, respectively. It was found that increasing the metal loading percentage from 0.5 wt% to 1 wt% causes the closure of a number of pore openings on the surface of the catalyst, which reduces the surface area. It also causes an increase in the activity of Lewis acids and rapid breakdown of the reactant hydrocarbons, thus resulting in a reduction in conversion and selectivity for isomers.

Keywords: Alumina Oxide, Bifunctional nanocatalyst, n-Heptane hydroisomerization, acidity, conversion.

دراسة تأثير التحميل المعدني النشط ضمن دعامة الكاما ألومينا على توزيع المنتج في التفاعلات الأيزومرية للهبتان العادي

الخلاصة:

في هذا البحث، تمت معالجة المحفز الحمضي أحادي الوظيفة γ-Al_2O_3 باستخدام معدن Pt بنسبة تتراوح من 0.5 إلى 1% بالوزن للحصول على محفز نانوي ثنائي الوظيفة يمثله Pt/Al_2O_3، بغرض زيادة مواقع المعدن النشط على سطحه. وبالتالي تعزيز تفاعلات الهدرجة/نزع الهيدروجين المهمة للغاية في تحفيز التفاعلات الأيزومرية بوجود الهيدروجين للهبتان العادي برقم أوكتان يساوي صفر. أجريت التجارب في وحدة تجريبية عند درجة حرارة 230 درجة مئوية وتحت ضغط 5 بار وبوجود غاز الهيدروجين لغرض إنتاج وقود هيدروكربوني مرغوب فيه ذو رقم أوكتان عالي. تم استخدام عدد من تقنيات التوصيف، بما في ذلك XRD وSEM وEDX وBET وFTIR، لتقييم الخواص الفيزيائية للعوامل الحفازة. تمت مقارنة السلوك التحفيزي للمحفزات المحضرة من خلال حساب تحويل الهيدروكربونات المتكونة والانتقائية تجاه توليد الأيزومرات في منتجات التفاعل. أشارت نتائج المقارنة إلى أن التحويل والانتقائية والإنتاجية تتبع الترتيب التالي وفقًا للكفاءة الحفزية للمحفزات: wt% Pt/Al_2O_3 0.5> 1wt% Pt/Al_2O_3 > γ-Al_2O_3 . تم العثور على أعلى نسبة تحويل وانتقائية وإنتاجية على سطح المحفز Pt/Al_2O_3 0.5wt% وكانت 62.50 و80.96 و50.60 وزن% على التوالي، في حين تم العثور على أقل نسب وزن للمنتجات على سطح المحفز الاساسي γ-Al_2O_3 غير محمل بالمعدن، وكانت 52.8 و67.7 و35.75 للتحويل والانتقائية والإنتاجية على التوالي. وقد وجد أن زيادة نسبة التحميل المعدني من 0.5% إلى 1% بالوزن تؤدي إلى إغلاق عدد من فتحات المسام الموجودة على سطح المحفز مما يقلل من مساحته السطحية. كما أنه يسبب زيادة في نشاط أحماض لويس وبالتالي يؤدي الى التكسر السريع للهيدروكربونات المتفاعلة، مما ينتج عنه انخفاض في التحويل والانتقائية للأيزومرات.

1. Introduction

The catalytic naphtha reforming reactor relies heavily on the reaction mechanism between the gaseous and solid phases of the catalyst, according to the principles of multiphase reactors. Therefore, the key factor in controlling the overall reaction mechanism in a reforming reactor is the heat and mass transfer rates at the catalyst surface [1] [2] [3]. Catalytic reforming typically involves a variety of different reactions, including the hydrocracking of paraffins to light hydrocarbons, hydroisomerization of paraffins and naphthenes, dehydrogenation of naphthenes to aromatics, dealkylation of alkylaromatics, and dehydrocyclization of paraffins [4] [5] [6]. All of these reactions have a big impact on the bifunctional method that happens on acid and metal sites. For reforming processes, Pt/Al_2O_3, $Pt\text{-}Ru/Al_2O_3$, $Pt\text{-}Re\text{-}Sn/Al_2O_3$, Pt/Zeolite, and Pt/Zirconia catalysts are the most frequently used industrial catalysts. From the point of view of heterogeneous reaction mechanisms, all the catalytic behaviors of these catalysts, as well as their deactivation rates, have a significant impact on the diffusion of reactant molecules that occurs within the solid catalysts [2] [6] [7].

The textures and pore sizes of catalysts have a significant impact on the heat and mass transfer processes that take place on their surfaces. In addition, nanocatalysts have great catalytic performance, high surface area, and strong resistance to deactivation [1] [6]. The production of high-octane gasoline with high-quality aromatics and branched hydrocarbons is usually the main

focus of continuous improvement of traditional- or nano-catalysts [8] [9] [10] [11]. Catalyst deactivation often results from the formation of unwanted compounds, coke formation being a prime example. Depending on the ability of the catalyst to resist deactivation processes, the performance of the catalyst in this case is modified. Moreover, the operating conditions and reaction rate have a significant impact on the performance, morphology, and crystal structure of the catalyst. To improve catalytic performance and stability, other metals are often used as promoter with catalysts [2] [12]. Due to its excellent thermal stability and important role in heterogeneous catalysis, platinum is a significant noble metal used for this purpose [13]. Improving catalytic activity using Pt-atoms atomically dispersed or in tiny clusters on supports has received much attention recently.

With more active sites and strong metal-support interaction, metal-based catalysts are used with atomically dispersed Pt-species [14] [15], and can significantly increase their catalytic activity and/or selectivity in a variety of reactions including oxygen reduction reactions, electrochemical catalytic reactions, and dehydrogenation/hydrogenation reactions [16] [17][18]. However, there is still much controversy about the fundamental roles that these structures, such as tiny Pt clusters or single atoms, play in alkane-reforming mechanisms [4] [19] [20] [21]. For instance, there are differences of opinion about how single Pt-atom affects the cyclization scheme. Since the coordination of the aromatic ring requires many Pt atoms prior to the hydrogenation, it is believed that the cycling process was not possible over single Pt-atom.

Possible catalytic reaction pathways for *n*-heptane in the presence of metallic (M) and acidic (A) sites are illustrated in Figure (1). The catalytic reaction pathway depends on the M/A ratio and the strength of each site. Commercially, Pt is supported on acidic alumina, which is used as catalysts in such hydroisomerization reactions. The role of alumina is as an acid site for the purpose of hydrocracking the reactant molecules, while the role of platinum metal is as a metal site for catalyzing hydrogenation/dehydrogenation reactions [22].

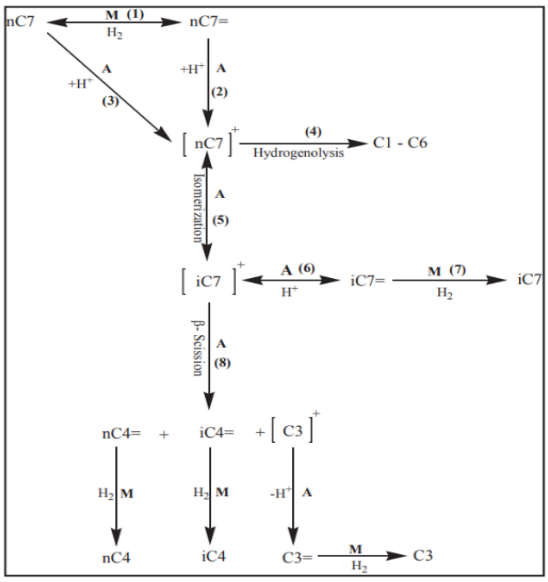

Fig. (1): Possible catalytic reaction pathways for *n*-heptane via acidic (A) and metallic (M) sites through the pores of the solid catalyst [22].

Kalashnikov studied the stability of the Pt/Al_2O_3 -BEA catalyst in the hydroisomerization of the heptane/benzene mixture model, and it was found that the investigated system is highly stable and does not deactivate for 53 hours of operation, while retaining its acidic properties and pore structure [23]. Hamied et al were investigated the kinetic modeling of light naphtha hydroisomerization over a Pt/Al_2O_3-Cl catalyst. They used a genetic algorithm stochastic optimization technique [24]. Medellin prepared and characterized the properties of Pt/Al_2O_3, $PtGe/Al_2O_3$, Pt/Al_2O_3–CeO, and $PtGe/Al_2O_3$–CeO_2 catalysts. The $PtGe/Al_2O_3$–CeO_2 catalyst showed high selectivity towards isomeric olefins in the *n*-heptane reforming and high resistance to self-deactivation [25]. Pashkov tested and modified Pt/Al_2O_3 catalyst with Group III (Ga) and Group IV (Ge, Ti, and Zr) elements in the reaction of propane and *n*-heptane. He found the conversion of propane and the concentration of C_{7+} were higher than those found on the unmodified Pt/Al_2O_3 sample [26]. René studied the effect of chlorine on the catalytic performance of the bifunctional catalysts Pt/Al_2O_3 and Pt/Al_2O_3/Zeolite Y with intimate ranges, and the observed differences between the behaviors of the catalysts were due to the addition of chlorine content to the catalytic performance of the Pt/Al_2O_3 references and mainly caused by the variety in the average platinum nano-particle size. The bifunctional catalysts and reference samples in *n*-heptane conversion were subsequently examined [27]. Mansour tested a high chlorinated alumina catalyst Pt/γ-Al_2O_3 (0.25 wt. % Pt) treated with two mixtures of CCl_4 /N_2 and CCl_4 /N_2 /H_2, for the hydroisomerization of the C_6 alkane diluted with hydrogen and performed with different H_2/HC ratios in the range of temperatures. It was found that there was superior conversion and

selectivity at 160°C and 120°C, and the highest octane number was observed at low space velocity (LHSV) of 1.2 h^{-1} [28].

This work aims to study the effect of loading γ-alumina (γ-Al_2O_3) nano-catalysts with platinum metal and its relationship to the catalytic behavior of the treated catalyst in *n*-heptane hydro-isomerization reactions. This is to determine the best type of catalyst loaded with metals that can be used in such a process. The results obtained for hydrocarbon conversion as well as the selectivity towards isomer from the use of monofunctional γ-Al_2O_3 and bifunctional γ-Pt/Al_2O_3 were carefully calculated and compared. In this study, the focus was on the Pt/Al_2O_3 nanocatalyst for the purpose of obtaining the optimal amount of metal that can be loaded onto the surface of the acid catalyst to reach the required balance in the dehydrogenation / hydrogenation processes necessary to produce isomers.

2. Experimental Work

2.1. Materials

Table (1) lists the types and sources of chemicals utilized in the experimental aspect of this study.

Table (1): Details regarding the materials purchased from commercial providers.

No.	Material	Structure	Company	Origin	Purity
1	Alumina Oxide Nanoparticles	γ-Al_2O_3 < 50 nm particle size	Fluka AG, Buchs SG.	Switzerland	99.9%~98%
2	Hydro-HexachloroPlatini Acid	$(H_2PtCl_6).6H_2O$	Direvo Industrial Biotechnology	Germany	99%
3	n-Heptane	$CH_3(CH_2)_5CH_3$	J.T.Baker	USA	99%
4	Hydrogen gases	H_2	Research and Development Center	Iraq	99.9%
5	Nitrogen gases	N_2	Research and Development Center	Iraq	99.9%
6	Deionized Water	H_2O	University of Technology - Baghdad	Iraq	99.99%

2.2. Characterization methods

The XRD Panalytical X'Pert Pro UK conducted the X-ray diffraction (XRD) analysis using a Cu Kα anode with λ=1.540 Å. The detector employed is called X'Celerator, which is a very fast X-ray detector based on Real Time Multiple Strip (RTMS) technology. TESCAN, MIRA3 XMU, Brno, Czech Republic, a scanning electron microscope (SEM), was used to determine the structural morphologies of the various catalysts. BRUKER Inspect S50, energy-dispersive X-ray

spectroscopy (EDX), was utilized to verify the elemental compositions on the surface of a specimen. Brunauer-Emmett-Teller (BET) technique was applied to calculate the BET-surface areas of the catalysts by means of using a HORIBA SA-9600 according to the gas adsorption-desorption isotherm phenomena at 77 K. SHIMADZU IR PRESTIGE-21 FTIR, AIM-8800 MICROSCOPE, Japan, Fourier transform infrared spectroscopy (FTIR), was employed to provide a view of the different bonds of chemicals and functional groups contained within the catalysts.

2.3. Bifunctional nanocatalyst preparation

In order to prepare the metal solution used for platinum loading, 1 g of the metal salt (i.e., H_2PtCl_6,$6H_2O$ Hexahydrate of Chloroplatinic Acid) is dissolved in 100 mL of deionized water using a magnetic mixer under 60°C for 1 h to be ready for the deposition of platinum metal on the support nanoparticles (γ-Al_2O_3). Following that, as seen in Figure (2), the produced metal solution was delicately dropped while being continuously stirred over the alumina aqueous solution. In order to get a homogenous solution, the resultant solution was agitated for 2 h at 80°C, adding the required amount of deionized water droplets. The solution was then allowed to dry overnight at 100°C in accordance with the metal loading method described in the literature [29]. The porous surface of the alumina nanoparticles was loaded with two specific concentrations of platinum metal (i.e., 0.5 and 1 wt%).

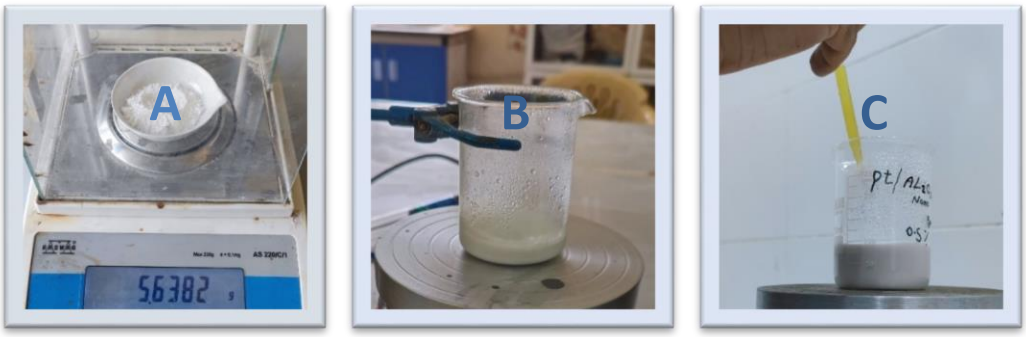

Fig. (2): (A) Weighing γ-Al_2O_3 nanocatalyst (B) γ-Al_2O_3 particles dissolution with distilled water (C) Loading with Pt-metal

2.3.1 Pelletizing of catalyst

As illustrated in Figure (3), the Pt/Al_2O_3 catalysts produced were pelletized by squeezing the sample powder into a small circular disk and applying a pressure of about 10 tons/m^2. The circular disk was then milled and sieved using a 125-300 μm mesh sieve to achieve the desired particle size of bifunctional nanocatalyst pellets with spherical and/or geometric shapes. The goal is to avoid a rapid drop in pressure within the reactor bed during *n*-hydroisomerization experiments.

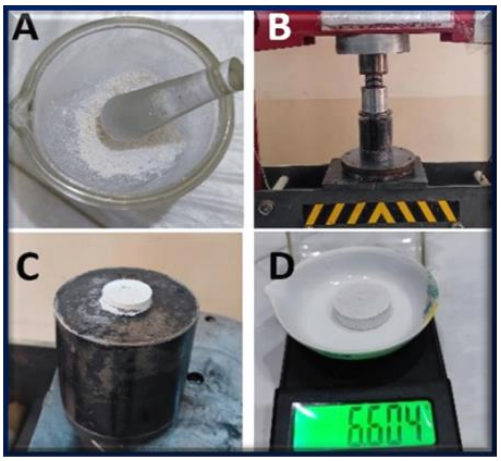

Fig. (3): (A) Catalyst powder, (B) Pressing device, (C) Casting equipment, and (D) Compressed disc of catalyst

2.4. Catalytic experimentation

As shown in Table (2), all nanostructured catalysts supported with various Pt-metal percentages were used in the *n*-heptane catalytic hydroisomerization reactions.

Table (2): Abbreviations of catalysts utilized in this study

NO.	CATALYST COD	CATALYSTS TYPE
1	Cat-1	Alumina Oxide: [γ-Al_2O_3]
2	Cat-2	[γ-Al_2O_3] loaded with 0.5%Pt: [0.5%Pt/Al_2O
3	Cat-3	[γ-Al_2O_3] loaded with 1%Pt: [1%Pt/Al_2O_3]

A fixed bed reactor constructed of stainless steel with an inner diameter of 10 mm and a length of 30 cm was filled with around 6 g of catalyst particles with sizes ranging from 125 to 300 μm. Two layers of ceramic spheres of 3 mm in diameter were utilized to fill the dead space in the reactor and stabilize the catalyst that was sandwiched between them. Before the reactants come into touch with the catalyst particles, these beads can assist in stabilizing the heating of the reactants. Prior to the start of the reaction, the metals that have been placed onto the catalyst surface undergo in situ reduction for a period of 3 h at a temperature of 350°C, a pressure of 5 bar, and a hydrogen flow rate of 5 L/h. Once the reactor reached a reaction temperature of 230°C, it was steadily cooled down. The *n*-heptane feed is then pushed into the liquid phase at a flow rate of 20 mL/h by the dosing pump – a positive displacement pump designed to inject a measured amount of liquid chemical into a flow of gas or steam. The feed stream eventually meets the hydrogen gas stream when it reaches at the catalyst bed together inside the reactor and begins the hydroisomerization

reaction. The reaction products were subsequently sent to a chromatography analyzer outfitted with a flame ionization detector (FID) so as to identify the hydrocarbon components that resulted from the reaction. This was done after the reaction products were condensed using a custom-built condenser that was operating at temperatures low enough to condense all of the resulting hydrocarbons (i.e., -15°C). The following equations were used to calculate conversion, selectivity, and yield [30].

$$Conversion = \frac{Initial\ moles\ of\ nC7 - Unreacted\ moles\ of\ nC7}{Initial\ moles\ of\ nC7} \times 100 \quad (1)$$

$$Selectivty = \frac{(Total\ moles\ of\ isomers)}{Initial\ moles\ of\ nC7 - Unreacted\ moles\ of\ nC7} \times 100 \quad (2)$$

$$Yield = \frac{Total\ moles\ of\ isomers}{Initial\ moles\ of\ nC7} \times 100 = [Conversion \times Selectivity] \times 100 \quad (3)$$

In order to test the catalytic behavior of the prepared Pt/Al_2O_3 catalysts, multiple experiments were performed inside the hydroisomerization rig that shown in the block diagram in Figure (4). The ideal parameters used in this study were determined experimentally after conducting a series of experimental tests under a range of operational conditions published in the literature for this type of reaction [31] [32] [33]. By calculating the difference between the weight of the liquid *n*-heptane that was introduced as a feed and the total condensed liquid products, material balancing was performed to measure the quantities of non-condensed gases produced (i.e., C_1 and C_2). It has been shown that light gases are almost negligible due to highly efficient condensation.

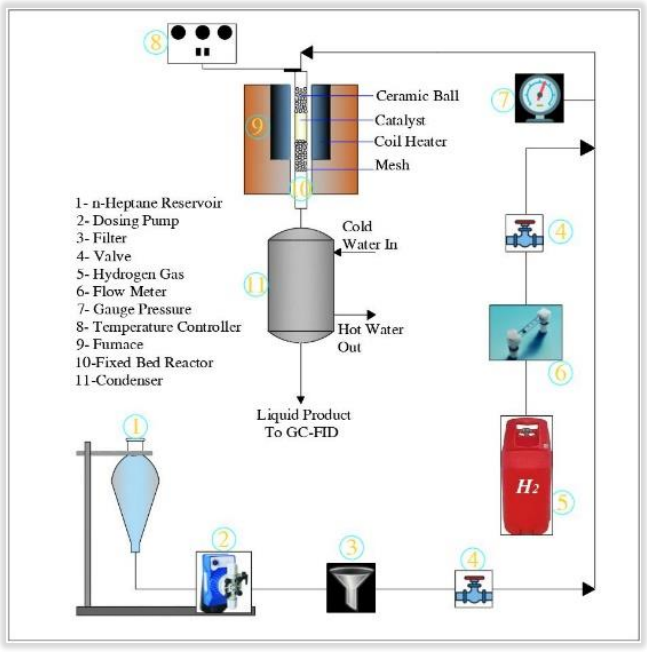

Fig. (4): Hydroisomerization rig

3. Results and Discussion

3.1. Characterization of the solid catalysts

The characteristics of the prepared nanocatalysts were analyzed using a variety of characterization techniques, including XRD, EDX, SEM, BET, and FTIR.

3.1.1 X-Ray diffraction (XRD) analysis

The structural frameworks of γ-Al_2O_3 & Pt/Al_2O_3 catalysts were examined using X-ray diffraction tests. The XRD patterns shown in Figure (5) were found to be similar to the equivalent XRD patterns of previous published studies [34][35].

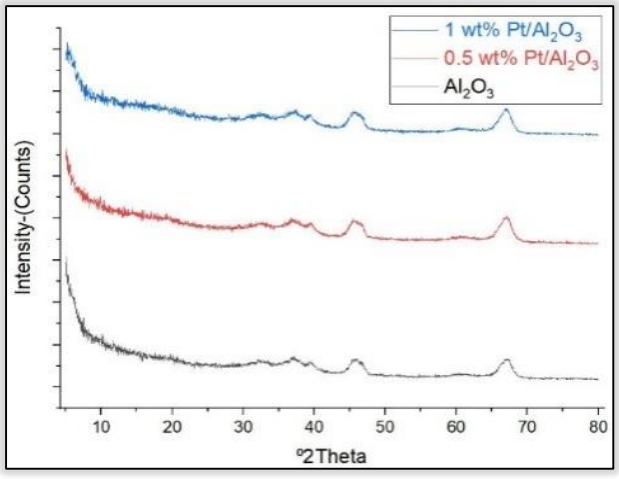

Fig. (5): XRD-patterns of γ-Al_2O_3 and Pt/Al_2O_3 of as-prepared catalysts loaded with two percentages of Pt-metal.

The structural characteristics of platinum metal-loaded alumina supports have an important role in determining the catalytic performance of catalysts. They are widely used as catalyst supports in the hydroisomerization process, and as a result their structural framework must be compatible with the standards lattice of the γ-Al_2O_3 catalyst [36][37]. The X-ray diffraction (XRD) patterns of both γ-Al_2O_3 and Pt/Al_2O_3 nanocatalysts have very similar patterns. Practically, all diffraction peaks were assigned identical to the standards Al_2O_3 peaks as shown in Figure (5). Due to the low amount of Pt (i.e., 0.5 & 1 wt%) in the mixture used to load the metal onto the catalyst surface, no clear distinction was seen on the diffraction peaks attributed to the Pt-species, and thus the diffraction patterns of the Al_2O_3 catalyst did not change after loading the metal on its surface [38].

3.1.2. Scanning electron microscope (SEM) analysis

Using scanning electron microscopy (SEM) at various magnifications, the surface morphologies of the Pt/Al_2O_3 catalysts loaded with two proportions of Pt-metals were examined. The SEM images are shown in Figure (6). No noticeable aggregation or deformation can be seen in the crystal forms, and they are all identical in crystal character with a semi-sharp edge. From SEM-analysis, the average particle size of the prepared nanocatalysts was determined to be about 11.03 nm of Al_2O_3, 14.15 nm of 0.5%wt Pt/Al_2O_3 and 15.65 nm of 1%wt Pt/Al_2O_3. In addition, it is noted that the particle size of the parent γ-Al_2O_3 catalyst is slightly smaller than that of the platinum-loaded nanocatalysts, which is due to the effective addition of Pt-metal atoms to the as-prepared catalyst particles and that is consistent with what has been documented by other authors [39][40].

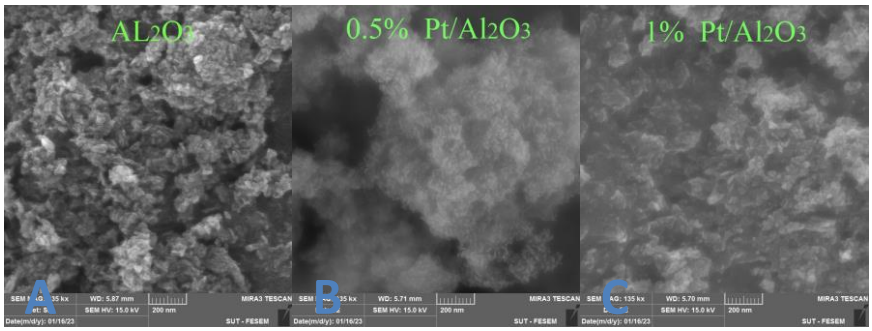

Fig. (6): SEM-images of (A) The parent γ-Al_2O_3 (B) and (C) γ-Al_2O_3 nanocatalysts loaded with (0.5 and 1) wt% of Pt-metal

3.1.3. Energy dispersive X-ray (EDX) analysis

The EDX spectra of alumina oxide and alumina oxide loaded with 0.5 and 1 wt% Pt-metal nanocatalyst are shown in Figure (7) and the material components on the surface of the catalysts

are investigated by this analysis. The platinum loading percentages on Al_2O_3 catalysts were practically the same in the range of 0.5 and 1 % by weight, according to the results of analysis of the amounts of each element. Due to the dispersion of Pt-atoms within the pores and cavities of the nanocatalyst, they are not accurately captured by this technique because it was created to scan only the percentage of elements present on the surface of the sample. Therefore, it is noted that there is a slight difference in the percentage of loaded Pt-metals calculated from the EDX analysis from the percentage required to be loaded, which is 0.5 and 1% by weight. Depending on the position of the spots selected during the EDX-test, a slight increase in the percentage of metal loaded may sometimes indicate agglomeration in the Pt distribution in certain regions rather than others. The other spectra of the EDX analysis show the weight percentages of the main nanocatalyst components, which are oxygen and aluminum with very small percentages of the other components appearing attributable to some impurities.

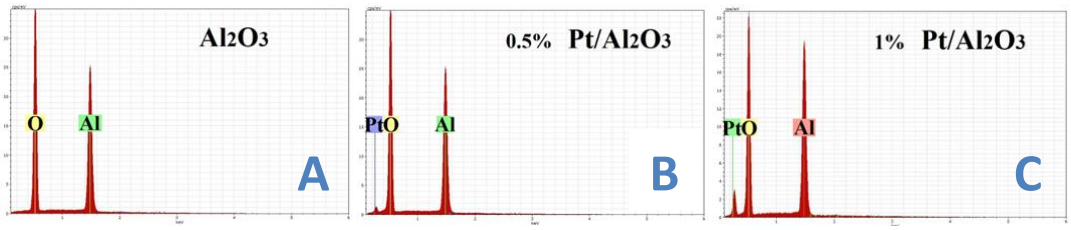

Fig. (7): EDX-spectra of (A) The parent γ-Al_2O_3 (B) and (C) γ-Al_2O_3 nanocatalysts loaded with (0.5 and 1) wt% of Pt-metal

3.1.4. BET-surface area analysis

The BET method was used to evaluate the catalyst surface area according to the physical adsorption of N_2-gas at 77 K. Before the BET measurement was conducted for 8 h and in order to get free of moisture and other contaminants, the catalyst samples were heated to roughly 350°C for out-gassing under vacuum pressure. The surface area and pore volume of the as-prepared catalysts are shown in Table (3).

Table (3): BET-surface area and pore volume of the parent γ-Al_2O_3 and the prepared Pt/Al_2O_3 nanocatalysts

No.	Catalysts Type	BET-surface Area (m^2/g)	Pore Volume (cm^3/g)
1	γ-Al_2O_3	177.961	0.967951
2	Al_2O_3 loaded with 0.5wt %I	132.122	0.718626
3	Al_2O_3 loaded with 1wt %P	124.756	0.678561

As a result of the presence of new active metal sites in the case of the Pt/Al_2O_3 catalyst, the results showed that the parent γ-Al_2O_3 catalyst had a slightly larger surface area and pore volume than those that were loaded with metals. In fact, these metal sites reduce the total surface area of the catalyst because they close part of the opening pores on the surface of the catalyst, which may prevent nitrogen gas molecules from entering the catalyst framework structure. The results of this study are consistent with what was reported in the literature [41], wherein it is noted that the surface area and pore volume of the catalyst decrease with the increase in the percentage of metals loaded on its surface.

3.1.5. Fourier-Transformed Infrared Spectra (FTIR) analysis

As illustrated in Figure (8), FTIR characterization technique is utilized to examine the functional groups and chemical bonds present within the parent γ-Al_2O_3 and the prepared Pt/Al_2O_3 nanocatalysts. The use of this test also aids in verifying the active loaded metal sites inside the structural framework of the catalyst to prove the success of the metal loading treatment and confirm the results of EDX-analysis.

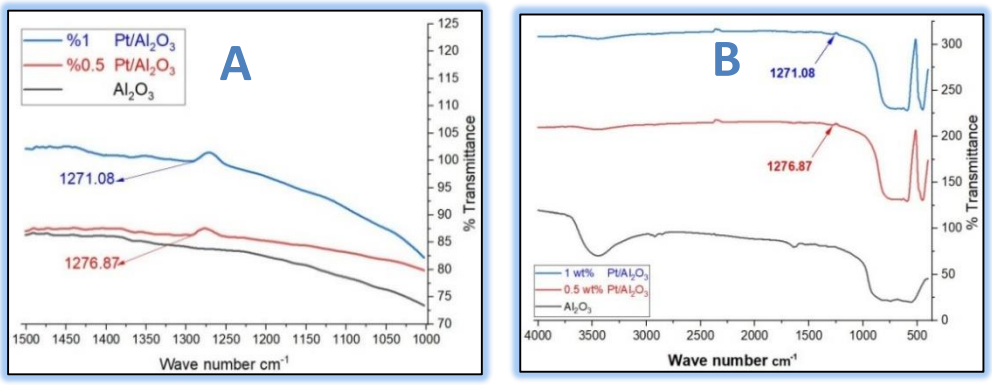

Fig. (8): FTIR spectra of the parent γ-Al_2O_3 and the prepared Pt/Al_2O_3 nanocatalysts (A) Wave number scale 1000-1500 cm^{-1} (B) Wave number scale 500-4000 cm^{-1}

The Pt/Al_2O_3 catalyst spectra show the existence of a wide band in the 1500-1000 cm^{-1} region that is connected to several electronic Pt-species, demonstrating that Pt exists in a variety of oxide species. After Pt loading, the vibration band at 3620 cm^{-1} has nearly completely vanished, indicating that Pt loading has decreased the acidity of the alumina sample. Since some Pt-atoms fit inside the Al_2O_3 pores, while others are present on the outer surface of the catalyst [42]. The most indicated broadband for 0.5%Pt loading is at 1276.87 cm^{-1} while the broadband of 1%Pt loading is at 1271.08 cm^{-1}.

3.2. The catalytic hydroisomerization reactions results

The conversion, selectivity, and yield were determined using experimental data of *n*-heptane hydroisomerization processes overs three nanostructured catalysts that have previously been reported in Table (2). The results of the experimental work are illustrated in Table (4).

Table (4): Experimental values of conversion, selectivity and yield

Catalysts	***Cat-1***	***Cat-2***	***Cat-3***
Conversion (wt%)	52.8	62.50	60.10
Selectivity (wt%)	67.7	80.96	78.78
Yield (wt%)	35.75	50.60	47.35

Figure (9) shows the catalytic performance of the catalysts used based on the data in Table (4), and it is clear that Cat-2 catalyst (i.e., 0.5wt% Pt/Al_2O_3) showed suitable catalytic behavior in *n*-hydroisomerization reactions, giving 62.5 wt% conversion and selectivity to isomers, including Isoheptane (i-C_7), 80.9 wt%. This conversion and selectivity are of the highest magnitude compared to the conversion selectivity obtained on the surfaces of the rest of the used catalysts. I*so*-heptane (*i*-C_7H_{16}), produced in a percentage of about 71.6 wt%, is usually the most important type of hydrocarbon component within the isomers formed during the *n*-heptane hydroisomerization reaction. The remaining resulting isomers are both *iso*-butane (*i*-C_4H_{10}) and *iso*-pentane (*i*-C_5H_{12}) and were generated in total percentages of approximately 28.4 wt%. These results are almost identical to those previously reported by Yunus et al [43]. It is expected that the change in the amount and distribution of the resulting product on the surface of the catalysts will be caused by the effect of the strength and distribution of the acid sites present on them, and that this change will also be affected by the operating variables of the process, as previously reported in the published literature [44]. Due to the thermal cracking of the reactant molecules that take place on the surface of the catalysts, especially during the beginning of the reaction, it is expected that heavy and light coke will be accumulated within the structural framework of the catalysts, this may cause the catalyst deactivation by covering acid sites and/or blocking pores. The amount of coke deposition can be calculated using TGA analysis and determining the weight loss of the catalysts. This process helps determine the temperature necessary to remove the coke from the catalyst and consequently reactivate it by burning under the influence of airflow, often at high temperatures [45]. In general, since hydrogen gas is present during the reactions to help accomplish the hydrogenation process, such as the *n*-heptane hydroisomerization reaction in this study, the amount of coke that builds up is greatly reduced, and the presence of H_2-gas also helps in activating

the hydrogenation/dehydrogenation reactions on the surface of the metals loaded on the catalyst. Hence, it activates the overall isomerization process [42] [46]. This is the reason for the clear increase in the production of isomers on the surface of the catalysts loaded with metal (i.e. Cat-2 and Cat-3) compared to the parent γ-Al_2O_3 catalyst (i.e. Cat-1) not loaded with Pt- metal. In addition, the speed at which linear paraffin chains (*n*-C), such as *n*-heptane, are broken tends to produce unsaturated olefins (C=) regardless of the increase in hydrocarbon conversion at the catalyst surface. In fact, it is very important that there are sufficient metal sites on the catalyst surface to maintain hydrogenation/dehydrogenation activity, which is necessary to produce significant rates of isomerization [47]. Isomer compounds with branched hydrocarbon chains and unsaturated olefins have a higher octane number than paraffins with linear hydrocarbon chains. Complete conversion of reactant hydrocarbons is often related to the level of reaction temperature required. Therefore, a more active catalyst with a lower reaction temperature is used. Reaching an appropriate balance between the acidic and metallic sites within the catalyst, as well as the hydroisomerization reaction temperatures, is a major challenge in this type of industrial process. Figure (10) shows the distribution of the spectra of hydrocarbons that appear in the *n*-hydroisomerization reaction on the surface of the used catalysts. It is noted that the lowest percentage of isomerized branched hydrocarbons was generated on the surface of the parent γ-Al_2O_3 catalyst, which is not loaded with platinum metal. On the other hand, a higher percentages of olefins and paraffins appeared on its surface. Moreover, the selectivity of the catalyst in catalytic reforming refers to the percentage of the desired product generated from the raw material (i.e., feedstock). The high yield of reformate at the appropriate octane number is good selectivity in motor fuel reforming. In other words, the selectivity of a catalyst refers to its ability to produce the desired products, which are often intermediate compounds. Conducting the reaction in the direction of the intended reaction is known as catalyst selectivity. Selectivity (i.e., branched hydrocarbons) is the ratio of the desired product (i.e., isomers), represented by *Wi*, to the total rate of transformation of the original substance, represented by *W*, and can be described by Equation 4 [48]:

$$S = \frac{Wi}{W} \qquad (4)$$

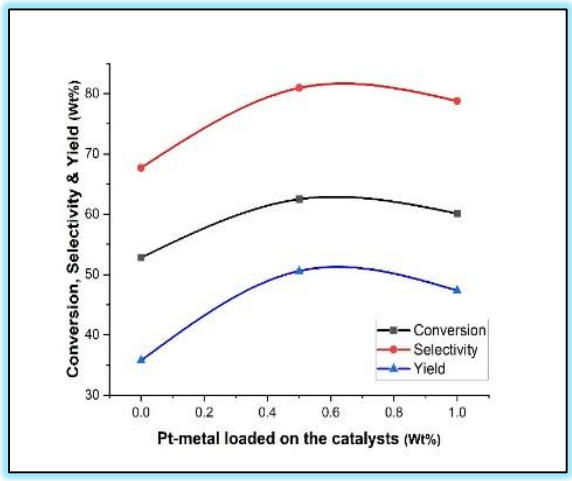

Fig. (9): Measurement of the catalytic performance of the parent γ-Al_2O_3 and the prepared Pt/Al_2O_3 nanocatalysts according to the ratio of platinum metal loaded on their surface.

According to the experimental results obtained, doubling the amount of platinum loaded on the catalyst surface reduces the conversion of hydrocarbons and the selectivity towards the isomer production, as observed when comparing the results of conversion and selectivity on the surfaces of Cat-2 or Cat-3 catalysts. The reason behind this is that excess metal can enhance the hydrogenolysis of hydrocarbons, increasing the formation of low molecular weight gases, and progressively reducing the production of isomers [49] [50] [51]. Accordingly, it is recommended not to load twice the amount of metal on the γ-Al_2O_3 catalyst. In addition, as previously pointed out, the presence of Pt atoms close to some catalyst pores can be attributed to the low conversion on the catalyst surface, when a large amount of Pt-metal is used. Because this leads to a decrease in the surface area or a complete closure of the opening pores on the surface of the catalysts, as shown in Table (3) previously, and this is consistent with what has been documented in other publications [51] [52].

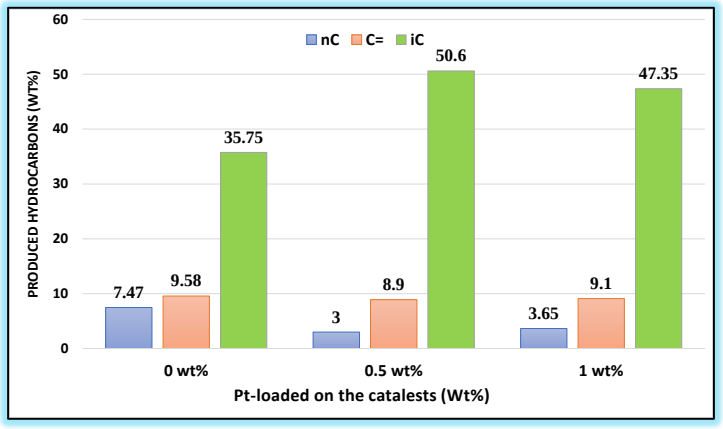

Fig. (10): The distribution of the spectra of hydrocarbons that appear in the *n*-hydroisomerization reaction on the surface of the used catalysts.

4. Conclusions

Hydroisomerization of *n*-heptane was catalyzed by adding Pt metal to alumina (γ-Al_2O_3) in two proportions (i.e., 0.5 and 1 wt%) at 230°C and 5 atm. It was found through the study that adding platinum metal to the surface of catalysts greatly enhances the hydrocarbons conversion as well as selectivity by increasing hydroisomerization towards the production of branched hydrocarbons with high octane numbers, which are the desired compounds in the produced fuel. In general, increasing the conversion and selectivity leads to increasing the yield of the materials produced from the reaction by reducing the amount of coke accumulated on the surface of the catalyst. The essential role that platinum metal plays in hydroisomerization reactions has been confirmed. It helps in the dehydrogenation process to convert naphthene into aromatic substances, and in the hydrogenolysis and dehydrogenation processes to convert paraffin into olefins, thus increasing the percentage of resulting isomers. As a result, both metal site function and acid site function are essential and both contribute sometimes individually and sometimes together to the hydroisomerization process. It was found through the study that doubling the amount of metal loaded on the surface of the catalyst from 0.5 to 1% has negative effects on conversion, selectivity, and yields because the increase in the atoms of loaded metal leads to the closure of the pores on the surface of the catalyst and reduces its total surface area. Metallic sites can also play a role as a Lewis acids sites and can accelerate the decomposition or breakdown of hydrocarbons rather than producing isomers. The conversion and selectivity can be increased by designing a precise balance for the amount of metallic and acidic sites on the catalyst surface, as well as adjusting the operating conditions, such as the applied pressure, reaction temperature, and the hydrogen gas supplied to the process, to avoid unwanted reactions that lead to an increase in by-products.

Acknowledgments

Appreciation goes to the institutions in the Republic of Iraq that directed and supported this research work, namely the Department of Chemical Engineering at the University of Technology affiliated with the Ministry of Higher Education and Scientific Research, as well as the Oil Research and Development Center affiliated with the Ministry of Oil.

Author Contribution Statement: Mohammed Khalil contributed to the research design, data processing, data analysis, data interpretation, literature review, drafting of the manuscript, and revision and proofreading. Zaidoon M. Shakor contributed to the conception of the research, research design, data analysis, data interpretation, drafting of the manuscript, and revision and proofreading. Bashir Y. Al-Zaidi contributed to the conception of the reseach, research design,

data interpretation, drafting of the manuscript, and revision and proofreading. Sattar J. Hussein contributed to the conception of the research, research design, data interpretation, drafting of the manuscript, and revision and proofreading. All authors have read and approved the final version of the manuscript.

References:

[1] A. Faridkhou, J.-N. Tourvieille, and F. Larachi, "Reactions, hydrodynamics and mass transfer in micro-packed beds—Overview and new mass transfer data", *Chemical Engineering and Processing: Process Intensification*, vol. 110, pp. 80–96, 2016. https://doi.org/10.1016/j.cep.2016.09.016.

[2] E. Blomsma, J. A. Martens, and P. A. Jacobs, "Isomerization and hydrocracking of heptane over bimetallic bifunctional PtPd/H-beta and PtPd/USY zeolite catalysts", *Journal of Catalysis*, vol. 165, no. 2, pp. 241–248, 1997. https://doi.org/10.1006/jcat.1997.1473.

[3] M. R. Asrami, B. Nejati, A. Tavasoli, and A. Karimi, "performance enhancement of pt-re/al 2 o 3 naphtha reforming nanocatalysts using microemulsion technique", *Petroleum & Coal*, vol. 58, no. 1, p. 56, 2016.

[4] Y. Zhu, Z. An, and J. He, "Single-atom and small-cluster Pt induced by Sn (IV) sites confined in an LDH lattice for catalytic reforming", *Journal of Catalysis*, vol. 341, pp. 44–54, 2016. http://dx.doi.org/10.1016/j.jcat.2016.06.004.

[5] D. Xu, S. Wang, B. Wu, B. Zhang, Y. Qin, C. Huo, L. Huang, X. Wen, Y. Yang, and Y. Li, "Highly dispersed single-atom Pt and Pt clusters in the Fe-modified kl zeolite with enhanced selectivity for n-heptane aromatization", *ACS Applied Materials & Interfaces*, vol. 11, no. 33, pp. 29858–29867, 2019. http://dx.doi.org/10.1021/acsami.9b08137.

[6] F. Aberuagba and A. A. Susu, "Nitrogen influence on aromatic selectivity during n-heptane reforming on fresh and deactivating platinum/alumina and platinum--rhenium/alumina catalysts", *Chemical Engineering and Processing: Process Intensification*, vol. 38, no. 3, pp. 179–196, 1999. https://doi.org/10.1016/S0255-2701(98)00081-6.

[7] J. Szczygieł, "Optimising the porous structure of heterogeneous reforming catalysts with a globular model of the grain", *Computers & Chemical Engineering*, vol. 35, no. 11, pp. 2334–2350, 2011. http://dx.doi.org/10.1016/j.compchemeng.2011.06.004.

[8] G. Zhang, X. Jin, J. Wang, M. Liu, W. Zhang, Y. Gao, X. Luo, Q. Zhang, J. Shen, and C. Yang, "Fe3+-Mediated Pt/Y Zeolite Catalysts Display Enhanced Metal--Bronsted Acid Interaction and Synergistic Cascade Hydrogenolysis Reactions", *Industrial & Engineering Chemistry Research*, vol. 59, no. 39, pp. 17387–17398, 2020. https://dx.doi.org/10.1021/acs.iecr.0c01971.

[9] Z. M. Shakor, A. A. AbdulRazak, and K. A. Sukkar, "A detailed reaction kinetic model of heavy naphtha reforming", *Arabian Journal for Science and Engineering*, vol. 45, pp. 7361–7370, 2020. https://doi.org/10.1007/s13369-020-04376-y.

[10] N. S. Ahmedzeki, B. A. Al-Tabbakh, M. B. Antwan, and S. Yilmaz, "Heavy naphtha upgrading by

catalytic reforming over novel bi-functional zeolite catalyst", *Reaction Kinetics, Mechanisms and Catalysis*, vol. 125, pp. 1127–1138, 2018. https://doi.org/10.1007/s11144-018-1432-y.

[11] C. Lin, H. Pan, Z. Yang, X. Han, P. Tian, P. Li, Z. Xiao, J. Xu, and Y. F. Han, "Effects of cerium doping on Pt--Sn/Al2O3 catalysts for n-heptane reforming", *Industrial & Engineering Chemistry Research*, vol. 59, no. 14, pp. 6424–6434, 2020. https://doi.org/10.1021/acs.iecr.9b05953.

[12] K. Li, Q Chang, J. Yin, C. Zhao, L. Huang, Z. Tao, Y. Yun, C. Zhang, H. Xiang, Y. Yang, and Y. Li, "Deactivation of Pt/KL catalyst during n-heptane aromatization reaction", *Journal of Catalysis*, vol. 361, pp. 193–203, 2018. https://doi.org/10.1016/j.jcat.2018.03.001.

[13] Z. Zhang, Y. Zhu, H. Asakura, B. Zhang, J. Zhang, M. Zhou, Y. Han, T. Tanaka, A. Wang, T. Zhang, and N. Yan, "Thermally stable single atom Pt/m-Al2O3 for selective hydrogenation and CO oxidation", *Nature Communications*, vol. 8, no. 1, p. 16100, 2017. https://doi.org/10.1038/ncomms16100.

[14] A. J. Therrien, A. J. R. Hensley, M. D. Marcinkowski, R. Zhang, F. R. Lucci, B. Coughlin, A. C. Schilling, J. McEwen, and E. C. H. Sykes, "An atomic-scale view of single-site Pt catalysis for low-temperature CO oxidation", *Nature Catalysis*, vol. 1, no. 3, pp. 192–198, 2018. https://doi.org/10.1038/s41929-018-0028-2.

[15] H. Fei *et al.*, "General synthesis and definitive structural identification of MN4C4 single-atom catalysts with tunable electrocatalytic activities", *Nature Catalysis*, vol. 1, no. 1, pp. 63–72, 2018. https://doi.org/10.1038/s41929-017-0008-y.

[16] H. Yan *et al.*, "Bottom-up precise synthesis of stable platinum dimers on graphene", *Nature Communications*, vol. 8, no. 1, p. 1070, 2017. https://doi.org/10.1038/s41467-017-01259-z.

[17] S. Vajda *et al.*, "Subnanometre platinum clusters as highly active and selective catalysts for the oxidative dehydrogenation of propane", *Nature Materials*, vol. 8, no. 3, pp. 213–216, 2009. http://www.nature.com/doifinder/10.1038/nmat2384.

[18] L. Liu, U. Diaz, R. Arenal, G. Agostini, P. Concepcion, and A. Corma, "Generation of subnanometric platinum with high stability during transformation of a 2D zeolite into 3D", *Nature Materials*, vol. 16, no. 1, pp. 132–138, 2017. http://dx.doi.org/10.1038/nmat4757.

[19] A. Arcoya, X. L. Seoane, and J. M. Grau, "Dehydrocyclization of n-heptane over a PtBa/Kl catalyst: reaction mechanism", *Applied Catalysis A: General*, vol. 284, no. 1–2, pp. 85–95, 2005. http://dx.doi.org/10.1016/j.apcata.2005.01.024.

[20] B. H. Davis, "Alkane dehydrocyclization mechanism", *Catalysis Today*, vol. 53, no. 3, pp. 443–516, 1999. https://doi.org/10.1016/S0920-5861(99)00136-4.

[21] P. MÉRIAUDEAU and C. NACCACHE, "Dehydrocyclization of alkanes over zeolite-supported metal catalysts: monofunctional or bifunctional route", *Catalysis Reviews*, vol. 39, no. 1–2, pp. 5–48, 1997. http://dx.doi.org/10.1080/01614949708006467.

[22] M. Hasan, A. M. Mohamed, and H. Al-Kandari, "Semi-industrial studies of Tungsten-based catalyst for hydroisomerization/hydrocracking of n-hexane and n-heptane", *Molecular Catalysis*, vol. 452, pp. 1–10, 2018. https://doi.org/10.1016/j.mcat.2018.03.017.

[23] I. M. Kalashnikov, E. A. Belopukhov, T. I. Gulyaeva, M. D. Smolikov, D. I. Kir'yanov, and A. S. Belyi, "A study on stability of the Pt/Al2O3--BEA catalyst in hydroisomerization of the n-heptane/benzene mixture", in *AIP Conference Proceedings*, vol. 2143, no. 1, p. 20027, 2019. https://doi.org/10.1063/1.5122926.

[24] R. S. Hamied, Z. M. Shakor, A. H. Sadeiq, A. A. A. Razak, and A. T. Khadim, "Kinetic Modeling of Light Naphtha Hydroisomerization in an Industrial Universal Oil Products Penex^{TM} Unit", *Energy Engineering*, vol.120, no.6, 2023. https://doi.org/10.32604/ee.2023.028441

[25] B. Medellin, R. Gomez, and G. Del Angel, "Effect of Ge and CeO_2 on Pt--Ge/Al_2O_3--CeO_2 reforming catalysts", *Catalysis Today*, vol. 150, no. 3–4, pp. 368–372, 2010. http://dx.doi.org/10.1016/j.cattod.2009.07.109.

[26] V. V. Pashkov, D. V. Golinskii, I. E. Udras, A. S. Kireeva, E. A. Paukshtis, K. S. Buyal'skaya, T. I. Gulyaeva, and A. S. Belyi, "Synthesis and characterization of the Pt/Al 2 O 3 systems modified with group III (Ga) and Group IV (Ge, Ti, and Zr) elements in the combined conversion of propane and n-Heptane", *Kinetics and Catalysis*, vol. 55, pp. 79–86, 2014. http://dx.doi.org/10.1134/S0023158414010091.

[27] R. A. van Alst and others, "The Influence of Chlorine on the Performance of Pt/Al2O3/Zeolite Y Bifunctional Catalysts", Master's thesis, Utrecht University, 2018.

[28] M. Jahangiri, F. Salehirad, and S. Alijani, "Preparation of Pt/Al2O3-Cl catalyst and investigation of operating variables effects on isomerization reaction", *Journal of Chemical and Petroleum Engineering*, vol. 52, no. 1, pp. 13–21, 2018. http://dx.doi.org/10.22059/jchpe.2018.233982.1198.

[29] E. V Benvenutti, L. Franken, C. C. Moro, and C. U. Davanzo, "FTIR study of hydrogen and carbon monoxide adsorption on Pt/TiO2, Pt/ZrO2, and Pt/Al2O3", *Langmuir*, vol. 15, no. 23, pp. 8140–8146, 1999. https://doi.org/10.1021/la990195s.

[30] L. O. Alemán-Vázquez, J. L. Cano-Domínguez, E. Torres-García, and J. R. Villagómez-Ibarra, "Industrial aplication of catalytic systems for n-heptane isomerization", *Molecules*, vol. 16, no. 7, pp. 5916–5927, 2011. https://doi.org/10.3390/molecules16075916.

[31] C. Huang, D. Han, L. Guan, L. Zhu, Y. Mei, D. He, and Y. Zu, "Bimetallic Ni-Zn site anchored in siliceous zeolite framework for synergistically boosting propane dehydrogenation", *Fuel*, vol. 307, p. 121790, 2022. https://doi.org/10.1016/j.fuel.2021.121790.

[32] S. Wang, M. Cao, S. Sun, H. Jiang, Y. Duan, X. Kong, and H. Wang, "Selective hydroisomerization of isobutane to n-butane over WO3-ZrO2 supported Ni-Cu alloy", *Fuel*, vol. 280, p. 118274, 2020. https://doi.org/10.1016/j.fuel.2020.118274.

[33] Y. Lyu, W. Zhan, X. Wang, Z. Yu, X. Liu, and Z. Yan, "Regulation of synergy between metal and acid sites over the Ni-SAPO-11 catalyst for n-hexane hydroisomerization", *Fuel*, vol. 274, p. 117855, 2020. https://doi.org/10.1016/j.fuel.2020.117855.

[34] J. Lee, E. J. Jang, D. G. Oh, J. Szanyi, and J. H. Kwak, "Morphology and size of Pt on Al2O3: The role of specific metal-support interactions between Pt and Al2O3", *Journal of Catalysis*, vol. 385, pp. 204–212, 2020. https://doi.org/10.1016/j.jcat.2020.03.019.

[35] P. Zhao, X. Li, W. Liao, Y. Wang, J. Chen, J. Lu, and M. Luo, "Understanding the Role of NbO x on Pt/Al2O3 for Effective Catalytic Propane Oxidation", *Industrial & Engineering Chemistry Research*, vol. 58, no. 48, pp. 21945–21952, 2019. https://doi.org/10.1021/acs.iecr.9b03916.

[36] C. Evangelisti, L. A. Aronica, M. Botavina, G. Martra, C. Battocchio, and G. Polzonetti, "Chemoselective hydrogenation of halonitroaromatics over $γ$-Fe2O3-supported platinum nanoparticles: The role of the support on their catalytic activity and selectivity", *Journal of Molecular Catalysis A: Chemical*, vol. 366, pp. 288–293, 2013. https://doi.org/10.1016/j.molcata.2012.10.007.

[37] S. Komhom, O. Mekasuwandumrong, P. Praserthdam, and J. Panpranot, "Improvement of Pd/Al_2O_3 c,atalyst performance in selective acetylene hydrogenation using mixed phases Al_2O_3 support," *Catalysis Communications*, vol. 10, no. 1, pp. 86–91, 2008. https://doi.org/10.1016/j.catcom.2008.07.039.

[38] Q. Bai, D. Li, L. He, H. Xiao, N. Sui, and M. Liu, "Solvent-free selective hydrogenation of o-chloronitrobenzene to o-chloroaniline over alumina supported Pt nanoparticles," *Progress in Natural Science: Materials International*, vol. 25, no. 3, pp. 179–184, 2015. https://doi.org/10.1016/j.pnsc.2015.05.005.

[39] R. Garidzirai, P. Modisha, I. Shuro, J. Visagie, P. van Helden, and D. Bessarabov, "The effect of Mg and Zn dopants on Pt/Al2O3 for the dehydrogenation of perhydrodibenzyltoluene", *Catalysts*, vol. 11, no. 4, p. 490, 2021. https://doi.org/10.3390/catal11040490.

[40] Z. Y. Nuru, L. Kotsedi, C. J. Arendse, D. Motaung, B. Mwakikunga, K. Roro, and M. Maaza "Thermal stability of multilayered Pt-Al2O3 nanocoatings for high temperature CSP systems", *Vacuum*, vol. 120, pp. 115–120, 2015. https://doi.org/10.1016/j.vacuum.2015.02.001.

[41] L. Silva, E. Luis, and C. Ana, "Sulphur-Tolerant Catalyst for Use in Water-Gas Shift Reactions, and Water-Gas Shift Process", *Pat. WO2016197211Al*, vol. 15, 2016.

[42] A. H. Samia, M. S. Mohammed, S. Faramawy, S. A. Ahmed, and H. B. Ahmed, "Influence of Pt nanoparticles modified by La and Ce oxides on catalytic dehydrocyclization of n-alkanes", *Egyptian Journal of Petroleum*, vol. 24, no. 2, pp. 163–174, 2015. https://doi.org/10.1016/j.ejpe.2015.05.007.

[43] Y. H. Khalaf, B. Y. S. Al-Zaidi, and Z. M. Shakour, "Experimental and Kinetic Study of the Effect of using Zr-and Pt-loaded Metals on Y-zeolite-based Catalyst to Improve the Products of n-heptane Hydroisomerization Reactions", *Orbital: The Electronic Journal of Chemistry*, vol. 14, no. 3, pp. 153–167, 2022. https://doi.org/10.17807/orbital.v14i3.17429.

[44] A. K. Dalai, R. Sethuraman, S. P. R. Katikaneni, and R. O. Idem, "Synthesis and characterization of sulfated titania solid acid catalysts", *Industrial & Engineering Chemistry Research*, vol. 37, no. 10, pp. 3869–3878, 1998. https://doi.org/10.1021/ie980091x.

[45] A. Al-Shathr *et al.*, "Experimental and kinetic studies of the advantages of coke accumulation over Beta and Mordenite catalysts according to the pore mouth catalysis hypothesis", *Catalysis Communications*, vol. 181, p. 106718, 2023. https://doi.org/10.1016/j.catcom.2023.106718.

[46] B. Y. Al-Zaidi *et al.*, "Hydroisomerisation and Hydrocracking of n-Heptane: Modelling and Optimisation Using a Hybrid Artificial Neural Network--Genetic Algorithm (ANN--GA)",

Catalysts, vol. 13, no. 7, p. 1125, 2023. https://doi.org/10.3390/catal13071125.

[47] H. A. Benesi, R. M. Curtis, and H. P. Studer, "Preparation of highly dispersed catalytic metals: Platinum supported on silica gel", *Journal of Catalysis*, vol. 10, no. 4, pp. 328–335, 1968. https://doi.org/10.1016/0021-9517(68)90147-4.

[48] M. Vadi, "Investigation of Activity and Selectivity of n-Heptane by Reforming Pt-Ta Catalyst Supported on γ-Alumina", *Journal Of Physical And Theoretical Chemistry*, vol. 7, no.1, pp. 49-52, 2010.

[49] M. E. Potter, J. J. M. Le Brocq, A. E. Oakley, E. B. McShane, B. D. Vandegehuchte, and R. Raja, "Butane isomerization as a diagnostic tool in the rational design of solid acid catalysts", *Catalysts*, vol. 10, no. 9, pp. 1–35, 2020. https://doi.org/10.3390/catal10091099.

[50] F. Ribeiro, C. Marcilly, and M. Guisnet, "Hydroisomerization of n-hexane on platinum zeolites. I. Kinetic study of the reaction on platinum/Y-zeolite catalysts: Influence of the platinum content", *Journal of Catalysis*, vol. 78, no. 2, pp. 267–274, 1982. https://doi.org/10.1016/0021-9517(82)90311-6.

[51] M. Saito and T. Iwasaki, "Isomerization of Pentanes on Platinum/Rare Earths-Hydrogen-Zeolite Y Catalysts", *Bulletin of The Japan Petroleum Institute*, vol. 18, no. 2, pp. 117–126, 1976. https://doi.org/10.1627/jpi1959.18.117.

[52] F. R. Ribeiro, "Use of platinum HY zeolite and platinum H mordenite in the hydroisomerization of n-hexane", *Zeolites: Science and Technology*, pp. 545–569, 1984. https://doi.org/10.1007/978-94-009-6128-9_20.